

# Collaborative Transportation of Cable-Suspended Payload using Two Quadcopters with Human in the loop

Pratik Prajapati, Sagar Parekh, and Vineet Vashista

**Abstract**—We study the problem of collaborative transportation of cable-suspended payload using two quadcopters. While previous works on transportation using quadcopters emphasize more on autonomous control and generating complex trajectory, in this paper a master-slave strategy is implemented where the master quadcopter is controlled by human and the slave quadcopter tries to stabilize the oscillations of the payload. Two quadcopters with a cable-suspended payload system is under-actuated with coupled dynamics and hence, manual control is difficult. We use Lagrangian mechanics on a manifold for deriving equations of motion and apply variation based linearization to linearize the system. We designed a Lyapunov based controller to minimize the oscillations of the payload while transportation, leading to an easier manual control of master quadcopter.

## I. INTRODUCTION

The recent years have seen an increasing trend in the use of Unmanned Aerial Vehicles (UAVs) in a wide range of applications including agriculture, payload transportation, surveillance, photography, etc. The use of UAVs to transport payloads can be utilized in various fields such as construction, military operations, disaster relief, delivering packages to name a few.

The payload can be attached rigidly to the quadcopter or it can be suspended using cables. In [1], a mechanical gripper was attached to the quadcopter for grasping and transporting payloads. The study [2] demonstrated the use of a robotic arm which was capable of picking and placing an object to transport from one place to another. However, the use of grippers or mechanical arms increases the overall inertia of the system, thereby reducing the agility of the quadcopter. On the other hand, with cable-suspended loads, the agility of the quadcopter is retained while still achieving the same task of picking and placing of the payload.

Load transportation with cable-suspended payload has been studied for a single quadcopter [3], [4], [5]. Shreenath et al. [6] showed that the system having an arbitrary number of quadcopters with a cable-suspended payload is differentially flat, and used this differential flatness property to generate dynamically feasible trajectories. A coordinate-free form of equations of motion was developed for multiple quadcopters with a cable-suspended payload to avoid singularities and ambiguities associated with local parameterization, and a controller was developed to follow a desired trajectory of the payload while the quadcopters maintain a prescribed

formation [7]. Gassner et al. [8] demonstrated a cable-suspended payload using two quadcopters by implementing a leader-follower scheme wherein the commands to the quadcopters are calculated based on the visual and inertial feedback obtained from onboard sensors.

The system of two quadcopters with a cable-suspended payload is under-actuated with a coupling between the dynamics of the suspended payload and that of the quadcopter which makes the control of overall system complicated. Previous works accentuate on developing control algorithms which can track the predefined trajectories of the payload. The scope of applications for the quadcopter can be further enhanced, by involving a human operator who can manipulate the desired trajectory during the flight. This would also enable the quadcopters-payload system to navigate through unknown environments without the need for mapping. However, the manual control of the system is difficult as the swinging of the suspended payload destabilizes the quadcopters.

Designing a controller in local coordinates using Euler angles exhibit singularities and derivation of equation of motion (EOM) becomes very cumbersome. So, in this paper, Lagrangian mechanics on manifold is used for derivation of EOM. Variation based linearization is used to linearize the non-linear system. A Lyapunov-based controller is developed on the linearized model which sends commands to the slave quadcopter to minimize the swings of the payload and also, try to stabilize cable oscillations while the master quadcopter follows the commands of a human operator through an RC remote control. The reduced oscillations of the payload results in better stability of the system making manual control easier as the operator needs to focus only on the motion of the master quadcopter without worrying about the dynamics of the system.

The paper is organized as follows. Section II derives the coordinate-free form of the EOM of the system. In section III, a controller is developed on the linearized system. Section IV discusses the experimental setup used for validation of the controller, and section V discusses the results of the experiment. Finally, concluding remarks are presented in section VI.

## II. DYNAMICAL MODEL OF THE SYSTEM

Consider a slender rod (payload) with mass  $m_L \in \mathbb{R}$  having moment of inertia  $J_L \in \mathbb{R}^{3 \times 3}$  suspended at each end from a quadcopter by cables as shown in Fig. 1. The position of the centre of gravity (CG) of the payload is given by  $x_L \in \mathbb{R}^3$  and its attitude is given by its rotation matrix,

Pratik Prajapati, Sagar Parekh, and Vineet Vashista\* are with the Human-Centered Robotics Lab at IIT Gandhinagar, Gujarat, India as a graduate student, an intern, and an assistant professor respectively. vineet.vashista@iitgn.ac.in

\*corresponding author

$R_L \in SO(3)$ , where  $SO(3)$  is the special orthogonal group defined as  $SO(3) = \{R \in \mathbb{R}^{3 \times 3} | RR^T = I, \det(R) = 1\}$ . The inertial frame is selected as  $\{e_1, e_2, e_3\}$  with the axis  $e_3$  pointing downward and the body-fixed frame attached to the payload is defined as  $\{b_1, b_2, b_3\}$ . The mass and moment of

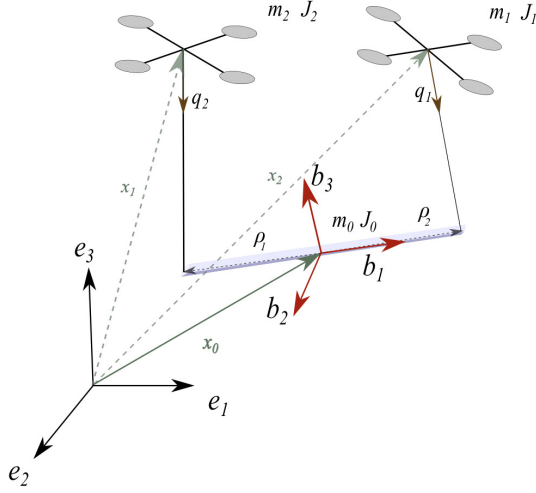


Fig. 1. Line diagram of two quadcopters transporting a cable-suspended payload.  $m_L$ ,  $J_L$ , and  $x_L$  represent mass, moment of inertia, and position vector of the payload.  $m_i$ ,  $J_i$ , and  $x_i$  ( $i = 1, 2$ ) represent the mass, moment of inertia, and position vectors of the quadcopters respectively. Position vectors are measured in the inertial frame  $(e_1, e_2, e_3)$ .  $q_i$  represent the attitude of the cable attached to the  $i^{th}$  quadcopter. Quadcopter 1 is treated as the master and quadcopter 2 is treated as the slave quadcopter.

inertia matrix of the  $i^{th}$  quadcopter are taken as  $m_i \in \mathbb{R}$  and inertia  $J_i \in \mathbb{R}^{3 \times 3}$  respectively. The cables used for connecting the payload to the quadcopter are considered to be mass-less and have a length  $l_i$  where  $i \in \{1, 2\}$ . Aggressive maneuvers of the quadcopter that can lead to slackness in the cable are not considered. The direction of the cables are measured outward from the quadcopter to the payload, and defined by the unit vector  $q_i \in \mathbb{S}^2$  where,  $\mathbb{S}^2 = \{q \in \mathbb{R}^3 | \|q\| = 1\}$ . The configuration manifold of the system is given by  $SO(3) \times \mathbb{R}^3 \times (SO(3) \times \mathbb{S}^2)^2$ .

The thrust force generated by the  $i^{th}$  quadcopter will be  $-f_i R_i e_3 \in \mathbb{R}^3$  with respect to the inertial frame, where  $f_i$  is the total magnitude of the thrust force produced by the  $i^{th}$  quadcopter and  $R_i \in SO(3)$  is the rotation matrix representing the attitude of the  $i^{th}$  quadcopter. In addition to this, the quadcopter also produces a moment  $M_i \in \mathbb{R}^3$  with respect to its body-fixed frame.

### A. Lagrangian

The kinematic equations for the quadcopters, cables, and payload are given as [9]

$$\dot{R}_i = R_i \hat{\Omega}_i \quad (1)$$

$$\dot{q}_i = \hat{\omega}_i q_i \quad (2)$$

$$\dot{R}_L = R_L \hat{\Omega}_L \quad (3)$$

where  $\omega_i \in \mathbb{R}^3$  is the angular velocity of the  $i^{th}$  cable which satisfies the condition  $q_i \cdot \omega_i = 0$ . Also,  $\Omega_L \in \mathbb{R}^3$

is the angular velocity of payload and  $\Omega_i \in \mathbb{R}^3$  is the angular velocity of the  $i^{th}$  quadcopter respectively in their corresponding body-fixed frame. The *hatmap*  $\hat{\cdot} : \mathbb{R}^3 \rightarrow SO(3)$  is defined as  $\hat{x}y = x \times y$  for all  $x, y \in \mathbb{R}^3$ . The inverse of the *hatmap* is called the *veemap* and is denoted by  $\vee : SO(3) \rightarrow \mathbb{R}^3$ . The position of the  $i^{th}$  quadcopter can be written as,

$$x_i = x_L + R_L \rho_i - l_i q_i \quad (4)$$

where  $\rho_i$  is the vector from the CG of the payload to the point where the  $i^{th}$  cable is attached to the payload. The total kinetic energy of the system is calculated as

$$\begin{aligned} \mathcal{T} = & \frac{1}{2} m_L \|\dot{x}_L\|^2 + \frac{1}{2} m_1 \|\dot{x}_1\|^2 + \frac{1}{2} m_2 \|\dot{x}_2\|^2 \\ & + \frac{1}{2} \Omega_L \cdot J_L \Omega_L + \frac{1}{2} \Omega_1 \cdot J_1 \Omega_1 + \frac{1}{2} \Omega_2 \cdot J_2 \Omega_2 \end{aligned} \quad (5)$$

and total potential energy of the system is calculated as

$$\mathcal{V} = -m_L g e_3 \cdot x_L - m_1 g e_3 \cdot x_1 - m_2 g e_3 \cdot x_2 \quad (6)$$

Using Eq. (5) and (6), the Lagrangian of the system can be calculated as  $\mathcal{L} = \mathcal{T} - \mathcal{V}$ .

### B. Euler-Lagrange Equations

The EOM of the system are derived with the help of Lagrangian mechanics on the two-spheres  $\mathbb{S}^2$  and special orthogonal group  $SO(3)$ . As did in [10], the infinitesimal variation of  $R_i$ ,  $i \in \{1, 2\}$  can be expressed in terms of the exponential map as

$$\delta R_i = \frac{d}{d\epsilon} \Big|_{\epsilon=0} R_i \exp(\epsilon \hat{\eta}_i) = R_i \hat{\eta}_i \quad (7)$$

where,  $\eta_i \in \mathbb{R}^3$ . and corresponding variation in the body angular velocity is given by,

$$\delta \Omega_i = \hat{\Omega}_i \eta_i + \dot{\eta}_i \quad (8)$$

Similarly, the infinitesimal variation of the  $q_i \in \mathbb{S}^2$  is given by,

$$\delta q_i = \frac{d}{d\epsilon} \exp(\epsilon \hat{\xi}_i) q_i = \hat{\xi}_i \times q_i \quad (9)$$

where,  $\xi_i \in \mathbb{R}^3$  which satisfies  $\xi_i \cdot q_i = 0$ . The corresponding infinitesimal variation in angular velocity is denoted as  $\delta \omega_i$ .

Using these variations, we derive the Euler-Lagrange equations of motion (EOM) of the system as follows

$$\begin{aligned} M_T \ddot{x}_L - \sum_{i=1}^2 m_i R_L \hat{\rho}_i \hat{\Omega}_L - M_T g e_3 + \sum_{i=1}^2 m_i R_L \hat{\Omega}_L^2 \rho_i \\ = \sum_{i=1}^2 u_i \end{aligned} \quad (10)$$

$$\begin{aligned}
& \left( \sum_{i=1}^2 m_i \hat{\rho}_i R_L^T \right) \ddot{x}_L + J_T \dot{\Omega}_L - \left( \sum_{i=1}^2 m_i l_i \hat{\rho}_i R_L^T \right) \ddot{q}_i \\
& - \left( \sum_{i=1}^2 m_i \hat{\rho}_i \hat{\Omega}_L R_L^T \right) \dot{x}_L + \sum_{i=1}^2 m_i l_i \hat{\rho}_i \hat{\Omega}_L R_L^T \dot{q}_i + \\
& \Omega_L \times (J_L \Omega_L - \sum_{i=1}^2 m_i \hat{\rho}_i^2 \Omega_L) - \sum_{i=1}^2 m_i g \hat{\rho}_i R_L^T e_3 \\
& = \sum_{i=1}^2 \hat{\rho}_i R_L^T u_i \quad (11)
\end{aligned}$$

$$\begin{aligned}
& -m_1 \hat{q}_1^2 \ddot{x}_L + m_1 \hat{q}_1^2 R_L \hat{\rho}_1 \dot{\Omega}_L - m_1 l_1 \ddot{q}_1 - m_1 l_1 \|\dot{q}_1\|^2 q_1 \\
& -m_1 \hat{q}_1^2 R_L \hat{\Omega}_L^2 \rho_1 + m_1 g \hat{q}_1^2 e_3 = -\hat{q}_1^2 u_1 \quad (12)
\end{aligned}$$

$$\begin{aligned}
& -m_2 \hat{q}_2^2 \ddot{x}_L + m_2 \hat{q}_2^2 R_L \hat{\rho}_2 \dot{\Omega}_L - m_2 l_2 \ddot{q}_2 - m_2 l_2 \|\dot{q}_2\|^2 q_2 \\
& -m_2 \hat{q}_2^2 R_L \hat{\Omega}_L^2 \rho_2 + m_2 g \hat{q}_2^2 e_3 = -\hat{q}_2^2 u_2 \quad (13)
\end{aligned}$$

$$J_1 \dot{\Omega}_1 - \Omega_1 \times J_1 \Omega_1 = M_1 \quad (14)$$

$$J_2 \dot{\Omega}_2 - \Omega_2 \times J_2 \Omega_2 = M_2 \quad (15)$$

where,

$$\begin{aligned}
M_T &= m_L + m_1 + m_2 \\
J_T &= J_L - \sum_{i=1}^2 m_i \hat{\rho}_i^2 \\
u_i &= -f_i R_i e_3
\end{aligned}$$

### III. METHODS

#### A. Controller Design for Simplified Model

Let the desired position of the payload be  $x_{L_d}$  and its desired attitude be  $R_{L_d} = I_{3 \times 3}$ . Similarly, the desired position of the cables (i.e.,  $q_{d_i}$ ) is chosen as vertically downward (i.e.,  $e_3$ ). The desired position of the  $i^{th}$  quadcopter will be given by

$$x_{i_d} = x_{L_d} + \rho_i - l_i e_3 \quad (16)$$

From EOM of the system, we can say that control input to the  $i^{th}$  quadcopter is  $f_i$  and it acts only along the corresponding third body fixed axis. As a result, the translational dynamics are under-actuated but, the rotational dynamics of the quadcopters are fully actuated. So, in this simplified model we have taken a fictitious control input  $u_i \in \mathbb{R}^3$  and assumed that the attitude of the quadcopters can be changed instantly. We have incorporated this attitude control of quadcopters in the following subsection.

As the dynamics of the system evolve on a nonlinear manifold, we can use variation based linearization in order to linearize the system about the desired trajectory as mentioned in [11]. The actual errors between the current trajectory and desired trajectory when system evolving on  $SO(3)$  can be given as [12]

$$e_{R_i} = \frac{1}{2} (R_d^T R_i - R_i^T R_d)^\vee \quad (17)$$

$$e_{\Omega_i} = \Omega_i - (R_i^T R_d) \Omega_d \quad (18)$$

where,

$$\Omega_i = R_i^T \dot{R}_i \text{ and } \Omega_d = R_d^T \dot{R}_d$$

If we assume that the orientation of the  $i^{th}$  quadcopter ( $R_i$ ) is very close to the desired orientation ( $R_d$ ) then we can take the state  $[\eta_i, \delta\Omega_i]^T$  as the error between the desired and actual states of the system evolving on  $SO(3)$ . We can write the error in states  $[\eta_i, \delta\Omega_i]^T$  as

$$\begin{bmatrix} \eta_i \\ \delta\Omega_i \end{bmatrix} \approx \begin{bmatrix} e_{R_i} \\ e_{\Omega_i} \end{bmatrix} = \begin{bmatrix} \frac{1}{2} (R_d^T R_i - R_i^T R_d)^\vee \\ \Omega_i - (R_i^T R_d) \Omega_d \end{bmatrix} \quad (19)$$

Similarly, assuming that the actual direction  $q_i$  of the  $i^{th}$  cable is very close to the desired direction  $q_{d_i}$ , we can take state  $[\xi_i, \delta\omega_i]^T$  as the errors between the desired and actual states of the system evolving on  $\mathbb{S}^2$ . The actual error  $e_{q_i}$  between  $q_i$  and  $q_{d_i}$  can be defined as [11],

$$e_{q_i} = \hat{q}_{d_i} q_i \quad (20)$$

$$e_{\omega_i} = \omega_i - (-\hat{q}_i^2) \omega_{d_i} \quad (21)$$

Same as before, we can write  $[\xi_i, \delta\omega_i]^T$  as,

$$\begin{bmatrix} \xi_i \\ \delta\omega_i \end{bmatrix} \approx \begin{bmatrix} e_{q_i} \\ e_{\omega_i} \end{bmatrix} = \begin{bmatrix} \hat{q}_{d_i} q_i \\ \omega_i - (-\hat{q}_i^2) \omega_{d_i} \end{bmatrix} \quad (22)$$

Eq. (19) and Eq. (22) are used for defining the errors for developing the control algorithm. At the equilibrium configuration of the system, the payload position and attitude are  $x_{L_d}$  and  $R_{L_d} = I_{3 \times 3}$  respectively and for the  $i^{th}$  cable  $q_{i_d} = e_3$ . The position of the  $i^{th}$  quadcopter is defined in Eq. (16) and its orientation is  $R_{i_d} = I_{3 \times 3}$ . All the translational and angular velocities of the payload, cables, and quadcopters are taken to be zero at the equilibrium configuration. The control input  $u_{i_d}$  to the  $i^{th}$  quadcopter is given by

$$u_{i_d} = -f_{i_d} R_{i_d} e_3 \quad (23)$$

where  $f_{i_d}$  is the magnitude of the total thrust generated by a single quadcopter and is equal to  $(\frac{m_L}{2} + m_i)g$ . The variation of payload position  $x_L$  is given by

$$\delta x_L = x_L - x_{L_d} \quad (24)$$

The variation of the payload attitude and cable attitude are defined as

$$\delta R_L = R_{L_d} \hat{\eta}_L = \hat{\eta}_L \quad (25)$$

$$\delta q_i = \xi_i \times e_3 \quad (26)$$

where,  $\eta_L \in \mathbb{R}^3$  and  $\xi_i \in \mathbb{R}^3$  satisfies  $\xi_i \cdot e_3 = 0$ . The variation of the angular velocity  $\omega_i$  is given by  $\delta\omega_i \in \mathbb{R}^3$  such that  $\delta\omega_i \cdot e_3 = 0$ . So, the third element of  $\xi_i$  and  $\delta\omega_i$  is zero for any equilibrium configuration. Hence, the state vector in the linearized model of the system contains  $C^T \xi \in \mathbb{R}^2$ , where  $C = [e_1, e_2] \in \mathbb{R}^{3 \times 2}$ . The variation in the control input can be taken as  $\delta u_i = u_i - u_{i_d}$ . The linearized equations of motion can be written as,

$$M\ddot{x} + Gx = B\delta u + g(x, \dot{x}) \quad (27)$$

Matrices  $M$ ,  $G$ , and  $B$  are omitted due to space constraint.  $g(x, \dot{x})$  represents the higher order terms. The state vector  $x \in \mathbb{R}^{10}$  and the input vector  $\delta u \in \mathbb{R}^6$  are given by,

$$x = [\delta x_L, \eta_L, C^T \xi_1, C^T \xi_2]^T$$

$$\delta u = [\delta u_1, \delta u_2]^T$$

After neglecting the higher order term  $g(x, \dot{x})$ , we can write linearized EOM in state space form as

$$\dot{z} = A_0 z + B_0 \delta u \quad (28)$$

where,  $z = [x, \dot{x}]^T \in \mathbb{R}^{20}$ .  $A_0 \in \mathbb{R}^{20 \times 20}$  and  $B_0 \in \mathbb{R}^{20 \times 6}$  are given by

$$A_0 = \begin{bmatrix} 0_{10 \times 10} & I_{10 \times 10} \\ -M^{-1}G & 0_{10 \times 10} \end{bmatrix}, B_0 = \begin{bmatrix} 0_{10 \times 6} \\ M^{-1}B \end{bmatrix}$$

We design a PD controller for the simplified model as,

$$\delta u_i = -K_p x - K_v \dot{x} \quad (29)$$

where  $K_p, K_v \in \mathbb{R}^{3 \times 10}$ . Putting this value of  $\delta u_i$  in Eq. (28), we have,

$$\dot{z} = A_c z$$

where  $A_c \in \mathbb{R}^{20 \times 20}$  is given as

$$A_c = \begin{bmatrix} 0_{10 \times 10} & I_{10 \times 10} \\ -M^{-1}(G + BK_p) & -M^{-1}BK_v \end{bmatrix}$$

To make the equilibrium asymptotically stable, we choose the gains  $K_p$  and  $K_v$  such that the matrix  $A_c$  is Hurwitz. Lyapunov based stability is mentioned in the appendix section A.

### B. Controller Design for the Full Dynamic Model

In section III-A, we ignored the attitude dynamics of the quadcopters and assumed a fictitious control input  $u_i$  which can generate thrust in all three directions independently. In this section, we design an attitude controller which can orient the third body-fixed axis of the quadcopter parallel to the direction of the control input designed previously.

The desired thrust force vector for the  $i^{th}$  quadcopter is defined as

$$F_i = u_{i_d} + \delta u_i \quad (30)$$

where,  $u_{i_d}$  is the total thrust vector for the  $i^{th}$  quadcopter at equilibrium condition. The commanded direction for the third body-fixed axis of the  $i^{th}$  quadcopter i.e.  $b_{3c_i} \in S^2$  is calculated as

$$b_{3c_i} = -\frac{F_i}{\|F_i\|}$$

The first body-fixed axis of the quadcopter can be defined arbitrarily as any continuous function of time,  $b_{1c_i}(t)$ . However, as the first and third body-fixed axis are normal to each other, the arbitrary command  $b_{1c_i}(t)$  cannot be followed exactly. But, the projection of  $b_{1c_i}(t)$  onto a plane normal to the third body-fixed axis can be followed. The second body-fixed axis can be calculated such that these three axes make an orthogonal coordinate frame. So, the commanded attitude of the quadcopter  $R_{c_i} \in SO(3)$  is given as

$$R_{c_i} = \begin{bmatrix} -\frac{(\hat{b}_{3c_i})^2 b_{1c_i}}{\|(\hat{b}_{3c_i})^2 b_{1c_i}\|} & \frac{\hat{b}_{3c_i} b_{1c_i}}{\|\hat{b}_{3c_i} b_{1c_i}\|} & b_{3c_i} \\ \frac{\hat{b}_{3c_i} b_{1c_i}}{\|\hat{b}_{3c_i} b_{1c_i}\|} & \frac{b_{3c_i}}{\|b_{3c_i}\|} & \end{bmatrix} \quad (31)$$

Finally, the control input  $f_i$  and  $M_i$  to each quadcopter can be calculated using the following expressions,

$$f_i = -F_i \cdot R_i e_3 \quad (32)$$

$$M_i = -K_{R_i} e_{R_i} - K_{\Omega_i} e_{\Omega_i} \quad (33)$$

where,  $e_{R_i} = \frac{1}{2}(R_{c_i}^T R_i - R_i^T R_{c_i})^\vee$ ,  $e_{\Omega_i} = \Omega_i - (R_i^T R_{c_i})\Omega_{c_i}$  and  $K_{R_i}$  and  $K_{\Omega_i}$  are positive constants. Due to space constraint the stability proof is not discussed in this paper but it is related to [13].

## IV. EXPERIMENTAL SETUP

This section describes the experimental setup used for validating the geometric controller developed in section III. The quadcopters used were PlutoX drones by Drona Aviation Pvt Ltd [14]. For estimating states of the quadcopters and the payload Vicon motion capture system was used [15]. The attitude and angular velocity of the quadcopters were determined from the on-board inertial measurement unit (IMU) while the attitude of the payload and cables was measured from the Vicon feedback data.

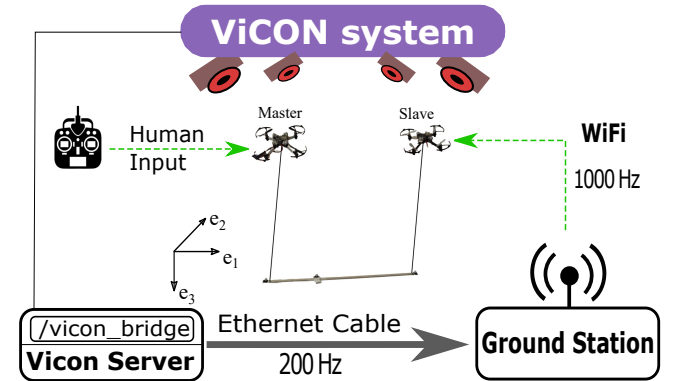


Fig. 2. Communication architecture of the system. The marker data from the Vicon system is accessed at the ground station via Ethernet cable at 200 Hz using the `/vicon_bridge` package [16] in ROS. The control inputs from the ground station are then sent to the slave quadcopter through WiFi at a frequency of 1000 Hz. The master quadcopter receives input commands from the human operator.

We use Robotics Operating System (ROS), which is a flexible framework for developing customized robotics applications, for developing the control algorithm. The communication between the Vicon system and the ground computing station happens via ethernet cables through ROS's `/vicon_bridge` package at a rate of 200 Hz. The quadcopters are equipped with an onboard PID attitude controller, and the control inputs to the quadcopters are in terms of desired roll, pitch, and yaw angles along with the throttle input. The values of desired attitude angles are calculated at the ground station and communicated to the quadcopters through WiFi at a rate of 1000 Hz. The communication architecture of the experimental setup is shown in Fig. 2. Each quadcopter has a maximum load-carrying capacity of 15g. An MDF strip of  $1.5cm \times 0.3cm \times 60cm$  having a mass of 24g is used as the payload. Each end of the payload is suspended from a point directly beneath the quadcopters with the help of cables of length 50cm.

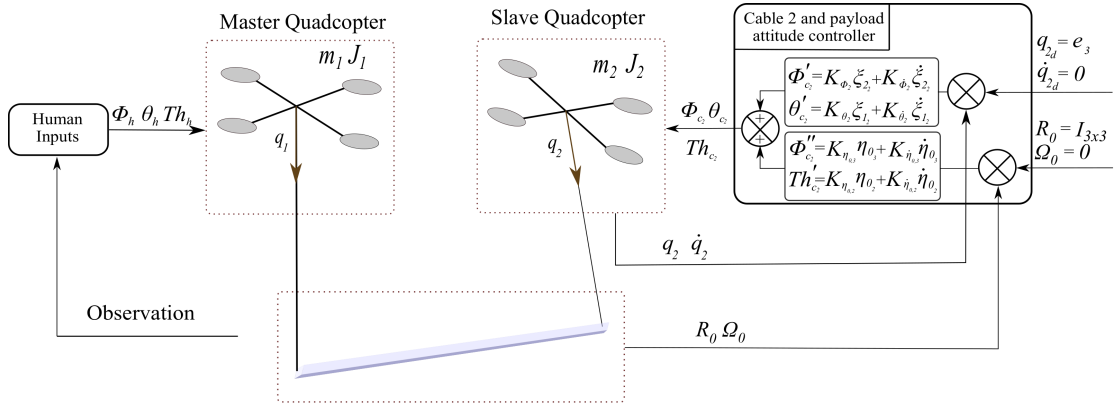


Fig. 3. Master Quadcopter is fully controlled by the human operator who commands it based on their observation of the system.  $\phi_h$ ,  $\theta_h$  and  $Th_h$  are the human commands. Slave quadcopter takes the feedback of the attitude and the angular velocities of cable 2 ( $q_2, \dot{q}_2$ ) and that of the payload ( $R_0, \Omega_0$ ).  $\phi'_{c2}$  and  $\phi''_{c2}$  are the commanded roll angles based on the errors in attitude of the cable 2 (i.e.  $\xi_{22}, \dot{\xi}_{22}$ ) and the errors in attitude of the payload (i.e.  $\eta_{02}, \dot{\eta}_{02}$ ) respectively.  $\theta'_{c2}$  is the commanded pitch angle calculated based on the errors in attitude of the cable ( $\xi_{12}, \dot{\xi}_{12}$ ),  $Th_{c2}$  is the commanded throttle, calculated using the payload attitude error ( $\eta_{02}, \dot{\eta}_{02}$ ). (Second subscript indicates the coordinate of the particular state.)

While experimenting, no yaw commands were given to the quadcopters to keep the yaw movement zero. The master quadcopter is fully controlled by the commands given by the human operator based on their observations of the system. The task of the slave quadcopter is to minimize the oscillations of the payload and cable 2 in order to stabilize entire system. The complete control architecture is depicted in Fig. 3. The commanded roll angle, pitch angle, and throttle to the slave quadcopter are calculated based on the following equations.

$$\phi_{c2} = \phi'_{c2} + \phi''_{c2} \quad (34)$$

$$\theta_{c2} = \theta'_{c2} \quad (35)$$

$$Th_{c2} = Th'_{c2} \quad (36)$$

where,

$$\phi'_{c2} = K_{\phi_2} \xi_{22} + K_{\dot{\phi}_2} \dot{\xi}_{22} \quad (37)$$

$$\theta'_{c2} = K_{\theta_2} \xi_{12} + K_{\dot{\theta}_2} \dot{\xi}_{12} \quad (38)$$

$$\phi''_{c2} = K_{\eta_{03}} \eta_{03} + K_{\dot{\eta}_{03}} \dot{\eta}_{03} \quad (39)$$

$$Th'_{c2} = K_{\eta_{02}} \eta_{02} + K_{\dot{\eta}_{02}} \dot{\eta}_{02} \quad (40)$$

As the master quadcopter moves arbitrarily in a particular direction, the translational position and velocity of the payload are not necessary as we only concern with the attitude of the payload. So, in control law, feedback gains for translational position and velocity of payload are not considered.

## V. RESULTS AND DISCUSSION

Due to movements of the master quadcopter, oscillations are induced in the cables and the payload. The desired orientation of the payload is taken as  $I_{3 \times 3}$  measured w.r.t the inertial frame and the desired cable attitude is along the  $e_3$  axis as discussed in section III.

From Fig. 4 (a), we can see that the slave quadcopter's position along  $e_2$  (y-position) and  $e_3$  (z-position) axes almost coincide with that of the master quadcopter while the position

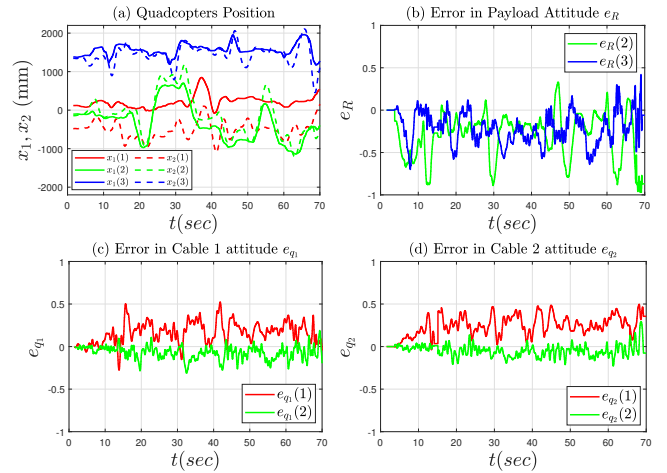


Fig. 4. (a) Translational movements of the Master quadcopter (indicated by the subscript 1) and Slave quadcopter (indicated by the subscript 2) w.r.t time, (b) Error in payload attitude  $e_R$  (c) Error in cable 1 attitude  $e_{q1}$  (d) Error in cable 2 attitude  $e_{q2}$ . (The number inside the parenthesis indicates the corresponding axis about which the value is measured.)

values in  $e_1$  (x-position) of the slave are around 600 mm (which is equal to the length of the payload) less than the position values in  $e_1$  of the master. So, the slave quadcopter tries to reach a position exactly behind the master quadcopter at the same altitude in order to achieve the desired attitude of the payload. In Fig. 4 (b), the error in attitude of the payload about the  $e_2$  and  $e_3$  axes are plotted. The error about  $e_2$  is due to the difference in the z-position of the two quadcopters while the error in attitude about  $e_3$  is due to the difference in the y-position of the quadcopters. As the master moves in y or z-direction, an error in the attitude of the payload about  $e_3$  or  $e_2$  respectively is produced, but the error goes on reducing until the next perturbation occurs due to the motion of the master quadcopter. Three markers are necessary to estimate the attitude of the payload. As the payload is taken as a strip, the third marker is placed at some offset from the line joining two markers which are placed at

each end of the strip. Since the payload is suspended at two endpoints, the payload oscillates about the axis passing from these two suspended points which lead to some inaccuracies in the payload attitude measurement. At 20 second, the y-position of the master quadcopter goes to around  $-1000$  mm, which creates an error in the payload attitude about  $e_3$  axis (i.e.,  $e_{R_L}$  about z-axis). The payload attitude controller will send commands to the slave quadcopter to compensate for these errors which is evident from the Fig. 4 (a) and (b) after 20 seconds.

Figure 4 (c) and (d) represent the attitude error in the cable 1 and cable 2 respectively. Since the third component of the cable attitude error is not contributing in control law, only the first two components of the cable attitude errors are plotted. More oscillations in cable attitudes are because of slave quadcopter is trying to minimize the oscillations of the payload during the movements of the master quadcopter.

It should be noted that the values of  $e_{R(2)}$  and  $e_{R(3)}$  are stabilized about a non-zero baseline (as shown in Fig. 4 (b)) because the payload is suspended using only two cables leading to some oscillations of the payload about its first body-fixed axis. Also, the markers on the payload are placed slightly offset from the point where the cables are attached to the payload leading to an offset in the cable attitude measurements as can be seen from Fig. 4 (c) and (d).

In the current work, a Vicon motion camera capture system was used to estimate the attitude of the payload and angular velocities. In future studies, experiments will be conducted in the outdoor settings where potentiometers will be used at the cable attachment point on the quadcopters as well as the payload for estimating the angular position and velocities of the cables. For estimating the payload attitude, an IMU can be attached to it. The main contribution of this work is to expand the scope of applications for a quadcopters by enabling human control under physical constraints.

## VI. CONCLUSIONS

At a time, the human operator cannot fly more than one quadcopters. But, if quadcopters are physically constrained using cable-suspended payload, it is possible to operate multiple quadcopters manually with the help of master-slave strategy. In this paper, we addressed the problem of two quadcopters transporting a cable-suspended payload using a master-slave approach; wherein a human operator commands the master quadcopter while the slave quadcopter tries to maintain the payload in the desired orientation for safe transportation. The experimental results show the effectiveness of the designed controller in minimizing the swing of the payload while reducing the error in the payload attitude. While experimentations, it is also noted that manual control of the entire system becomes much easier. Hence, the applicability of the two quadcopter system can be improved by keeping a human in the loop.

## APPENDIX

### A. Lyapunov stability for simplified model

Consider a quadratic form of the lyapunov function as follows,

$$V(z) = z^T P z \quad (41)$$

where,  $P$  is a real, symmetric, positive definite matrix. The derivative of lyapunov function will be,

$$\dot{V}(z) = z^T [A_c^T P + P A_c + \dot{P}] z \quad (42)$$

For the system to be asymptotically stable,  $\dot{V}$  must be negative definite and for that matrix equation  $A_c^T P + P A_c + \dot{P} = -Q$  must be true for some positive definite matrix  $Q$ . So, if we can find matrix  $P$  that satisfies the above equation then it guarantees asymptotic stability of the system.

## REFERENCES

- [1] Daniel Mellinger, Quentin Lindsey, Michael Shomin, and Vijay Kumar. Design, modeling, estimation and control for aerial grasping and manipulation. In *2011 IEEE/RSJ International Conference on Intelligent Robots and Systems*, pages 2668–2673. IEEE, 2011.
- [2] Suseong Kim, Seungwon Choi, and H Jin Kim. Aerial manipulation using a quadrotor with a two dof robotic arm. In *2013 IEEE/RSJ International Conference on Intelligent Robots and Systems*, pages 4990–4995. IEEE, 2013.
- [3] Koushil Sreenath, Nathan Michael, and Vijay Kumar. Trajectory generation and control of a quadrotor with a cable-suspended load-a differentially-flat hybrid system. In *2013 IEEE International Conference on Robotics and Automation*, pages 4888–4895. IEEE, 2013.
- [4] Koushil Sreenath, Taeyoung Lee, and Vijay Kumar. Geometric control and differential flatness of a quadrotor uav with a cable-suspended load. In *52nd IEEE Conference on Decision and Control*, pages 2269–2274. IEEE, 2013.
- [5] Koushil Sreenath, Taeyoung Lee, and Vijay Kumar. Geometric control and differential flatness of a quadrotor uav with a cable-suspended load. In *52nd IEEE Conference on Decision and Control*, pages 2269–2274. IEEE, 2013.
- [6] Koushil Sreenath and Vijay Kumar. Dynamics, control and planning for cooperative manipulation of payloads suspended by cables from multiple quadrotor robots. *rn*, 1(r2):r3, 2013.
- [7] Taeyoung Lee, Koushil Sreenath, and Vijay Kumar. Geometric control of cooperating multiple quadrotor uavs with a suspended payload. In *52nd IEEE conference on decision and control*, pages 5510–5515. IEEE, 2013.
- [8] Michael Gassner, Titus Cieslewski, and Davide Scaramuzza. Dynamic collaboration without communication: Vision-based cable-suspended load transport with two quadrotors. In *2017 IEEE International Conference on Robotics and Automation (ICRA)*, pages 5196–5202. IEEE, 2017.
- [9] Farhad A Goodarzi and Taeyoung Lee. Stabilization of a rigid body payload with multiple cooperative quadrotors. *Journal of Dynamic Systems, Measurement, and Control*, 138(12):121001, 2016.
- [10] Taeyoung Lee. *Computational Geometric Mechanics and Control of Rigid Bodies*. PhD thesis, 2008.
- [11] Guofan Wu and Koushil Sreenath. Variation-based linearization of nonlinear systems evolving on  $SO(3)$  and  $S^2$ . *IEEE Access*, 3:1592–1604, 2015.
- [12] Taeyoung Lee. Geometric tracking control of the attitude dynamics of a rigid body on  $SO(3)$ . In *Proceedings of the 2011 American Control Conference*, pages 1200–1205. IEEE, 2011.
- [13] Taeyoung Lee, Melvin Leok, and N Harris McClamroch. Nonlinear robust tracking control of a quadrotor uav on  $SE(3)$ . *Asian Journal of Control*, 15(2):391–408, 2013.
- [14] Plutox quadcopter, drona aviation pvt ltd. <https://www.dronaaviation.com>.
- [15] Vicon motion capture systems. <https://www.vicon.com>.
- [16] Vicon bridge ros package. [https://github.com/ethz-asl/vicon\\_bridge.git](https://github.com/ethz-asl/vicon_bridge.git).